Acta Geophysica
https://doi.org/10.1007/s11600-024-01403-6

RESEARCH ARTICLE - APPLIED GEOPHYSICS

Optimal processing of single-channel sparker marine seismic data

Aslıhan Nasıf[1]

Received: 21 November 2023 / Accepted: 13 June 2024
© The Author(s) 2024

Abstract
Single-channel sparker seismic reflection systems are currently preferred in offshore geo-engineering studies due to their cost-effectiveness, ease of use in shallow areas, their high-resolution data, and straightforward data processing. However, the distinctive characteristics of sparker data introduce specific challenges in the processing of single-channel seismic datasets. These include (i) unavailability of the stacking process for single-channel seismic data, (ii) inability to derive subsurface velocity distribution from single-channel seismic profiles, (iii) limitations imposed by ghost reflections and bubble effects as well as random noise amplitudes, and (iv) the suitability of only predictive deconvolution for suppressing multiple reflections. Applications demonstrate that the inability to apply the stacking process to single-channel seismic data poses a significant challenge in suppressing both random and coherent noise, and increasing the signal-to-noise (S/N) ratio. The F-X prediction filter has proven highly effective in mitigating random noise in sparker data. Appropriate determination of operator length and prediction lag parameters allows predictive deconvolution to effectively suppress multiple reflections, despite some residual multiple amplitudes in the output. Spiking deconvolution significantly eliminates ghost reflections and bubble effects, enhancing temporal resolution by eliminating the ringy appearance of the input signal. Trace mixing is a crucial data processing step for enhancing sparker data resolution. The method can be applied as weighted mix for random noise suppression or as trimmed mix for suppressing high-amplitude spike-like noises. This study incorporates a comprehensive analysis of the various noise components embedded in sparker seismic data. It delineates the processing flow and parameters utilized to effectively mitigate these specific noise types.

Keywords Sparker source · Seismic data processing · Noise suppression · Single-channel marine seismic

Introduction

In contemporary marine seismic data acquisition studies, the standard seismic source utilized is the air gun, which operates by the technique of sudden and high-pressure air discharge at specified time intervals (shot intervals) into the water to generate seismic signals. Air guns, which are also employed by the petroleum industry today, are recognized as reliable, repeatable sources requiring minimal maintenance, producing seismic signals within the approximate range of 5–250 Hz (Dragoset 2000).

In addition to air guns, sparker seismic systems are today commonly employed in single-channel marine seismic studies. In these systems, a high-voltage electrical current is transmitted to conductive tips, referred to as electrodes, immersed in seawater. Sparker sources induce the discharge of a high-voltage electrical current between electrodes in a conductive liquid (saline water), causing the evaporation of water due to the discharge. This process leads to the expansion and collapse of bubbles because the static pressure is smaller than the vapor pressure of the liquid (Duchesne et al. 2007; Pei et al. 2019). The collapse of these bubbles generates seismic waves (e.g., Verbeek and McGee 1995).

Standard sparker sources typically generate high-resolution seismic signals in the range of 50–2000 Hz with source wavelet durations of 1–5 ms. In recent times, sparker systems with very short receiver cables (streamers) containing 24 or 48 channels have been utilized. However, the sparker systems are generally employed for single-channel seismic data acquisition using single-channel

Edited by Prof. Gulan Zhang (ASSOCIATE EDITOR) / Prof. Gabriela Fernández Viejo (CO-EDITOR-IN-CHIEF).

✉ Aslıhan Nasıf
aslihan.nasif@deu.edu.tr

[1] Institute of Marine Sciences and Technology, Dokuz Eylül University, Haydar Aliyev Street, No: 100, 35340 İnciraltı, İzmir, Türkiye

Published online: 28 June 2024

streamers. Typically, resolution is inversely proportional to power of sparker sources and ranges between 25 cm and 3 m. High-powered sparker systems can achieve penetration depths exceeding 500 m from the seafloor (Mosher and Simpkin 1999; Duchesne et al. 2007). They can be safely and effectively used even in relatively shallow waters and on small vessels for marine geo-engineering studies in shallow shelf areas, revealing potential geohazards such as faults, shallow gas accumulations, and landslides (e.g., Trabant 1984; Huang et al. 2015; Zheng et al. 2021). However, limitations in very shallow waters and the substantial influence of sea conditions on data quality constitute significant drawbacks.

When compared to multi-channel data acquisition, single-channel data collection is relatively simple and more cost-effective in terms of equipment and data acquisition techniques. The processing of collected data is also less complicated. However, two crucial advantages of multi-channel seismic data acquisition are not utilized in single-channel seismic studies: obtaining the seismic velocity distribution of the subsurface and the effectiveness of the stacking process in noise suppression. Indeed, subsurface velocity distribution through velocity analysis methods can only be obtained by collecting multi-channel seismic data (Dondurur 2018). Moreover, the stacking process itself is one of the most effective data processing steps in suppressing associated noise such as random and some coherent noise such as multiple reflections, and stacking can only be performed in the case of multi-channel seismic data acquisition.

The theoretical framework of some data processing methods, particularly for the suppression of multiple reflections, is generally applicable to multi-channel seismic data, and considerable effort may be required for the elimination of multiple reflections and random noise in single-channel sparker seismic data (Santos et al. 2021; Wang et al. 2019; Kluesner et al. 2019; Wu et al. 2020; Duchesne et al. 2007). Additionally, the use of high-current and high-voltage electrical signals by the sparker source may lead to the widespread observation of spike-like transient and high-amplitude noise in the seismic data. Therefore, the data processing steps and associated parameters applied to enhance the signal-to-noise ratio (S/N) in sparker data differ from those applied to multi-channel seismic data processing steps and parameters (e.g., Santos et al. 2021; Duchesne et al. 2007; Jones 2013; Herman et al. 2017; Pei et al. 2019). For instance, sparker sources produce mixed-phase rather than minimum-phase signals (Alessandrini and Gasperini 1989; Kluesner et al. 2019; Verbeek and McGee 1995; Mosher and Simpkin 1999; Duchesne et al. 2007), and this characteristic implies that the deconvolution process applied to sparker data may not always be successful. Therefore, the seismic data processing techniques for sparker sources have become a subject of research in the field of high-resolution marine seismic investigations in recent years (Kong et al. 2012; Yang et al. 2022).

The seismic data processing industry has traditionally focused on the processing of multi-channel seismic reflection data, with extensive theoretical and practical studies conducted in this regard. The purpose of this study is to elucidate the details of processing single-channel sparker seismic data, which differ in data processing steps and parameters compared to the processing of multi-channel seismic data. The content of the study involves a detailed explanation and application of each processing step and its corresponding parameters employed in the processing of sparker data. Additionally, the study analyzes the types of noise observed in sparker seismic data with seismic data examples.

Noise in sparker data

"Noise" is defined as all types of unwanted events in the seismic data (Yılmaz 2001; Dondurur 2018; Birinci et al. 2023). If noise can be distinguished from the signal based on one of its specific characteristics such as propagation direction, slope, velocity, or frequency band, it may be possible to suppress the amplitude of that specific noise through data processing methods (Yılmaz 2001; Dondurur 2018).

Operational noise

Operational noise originates directly from the hydrodynamic motion, engine, machinery, and propeller of the vessel conducting the seismic operations. Noise from the machinery on the vessel is generated by the transfer of vibrations from main engines, generators, or seismic air compressors into the water (Dondurur 2018). Operational noise can generally have an impact on the near-offset traces of seismic data. In practice, operational noise can become pronounced in late arrivals, where gain recovery processes increase noise amplitudes.

To minimize the influence of operational noise on the sparker streamer, tow distance from the seismic vessel should be as large as possible. Nevertheless, the towing distance in sparker acquisition is generally much shorter than the distance applied in multi-channel seismic data acquisition. Consequently, operational noise may manifest as linear events in late arrivals in sparker data and can be mitigated with an appropriate frequency–wavenumber (f-k) filter. Additionally, the wake from the propeller can have a disruptive effect on the shape of the signal generated by the sparker source near the water surface and the amplitude of the signal detected at the streamer. Therefore, to avoid interference from the wake, the sparker source and streamer are typically towed at both sides of the vessel during the data acquisition.

Swell noise

This type of noise originates from waves caused by wind on the sea surface. Due to the sensitivity of hydrophones to pressure changes, it appears in the data as successive high-amplitude and low-frequency positive and negative noise bands (Birinci et al. 2023; Dondurur 2018; Dondurur and Karslı 2012; Elboth et al. 2009; Bekara and van der Baan 2010). The most significant characteristic of swell noise is its high-amplitude and low-frequency content.

In sparker studies, since the receiver cable is towed from the sea surface (or very close to the surface), the amplitude of swell noise can become much more pronounced in sparker data. Despite its high amplitude, it can be easily distinguished from reflection amplitudes because it has different frequency contents compared to reflection signals (Fig. 1a). The dominant frequency of this noise in sparker data is generally below 50 Hz, and a suitable band-pass filter can be applied to remove most of the noise from the data. While this results in the removal of low-frequency signal amplitudes in seismic data, the amplitudes of deep reflections are not significantly affected, because the penetration of high-resolution sparker signal is already low and is typically limited to 200 m below the seafloor. However, the

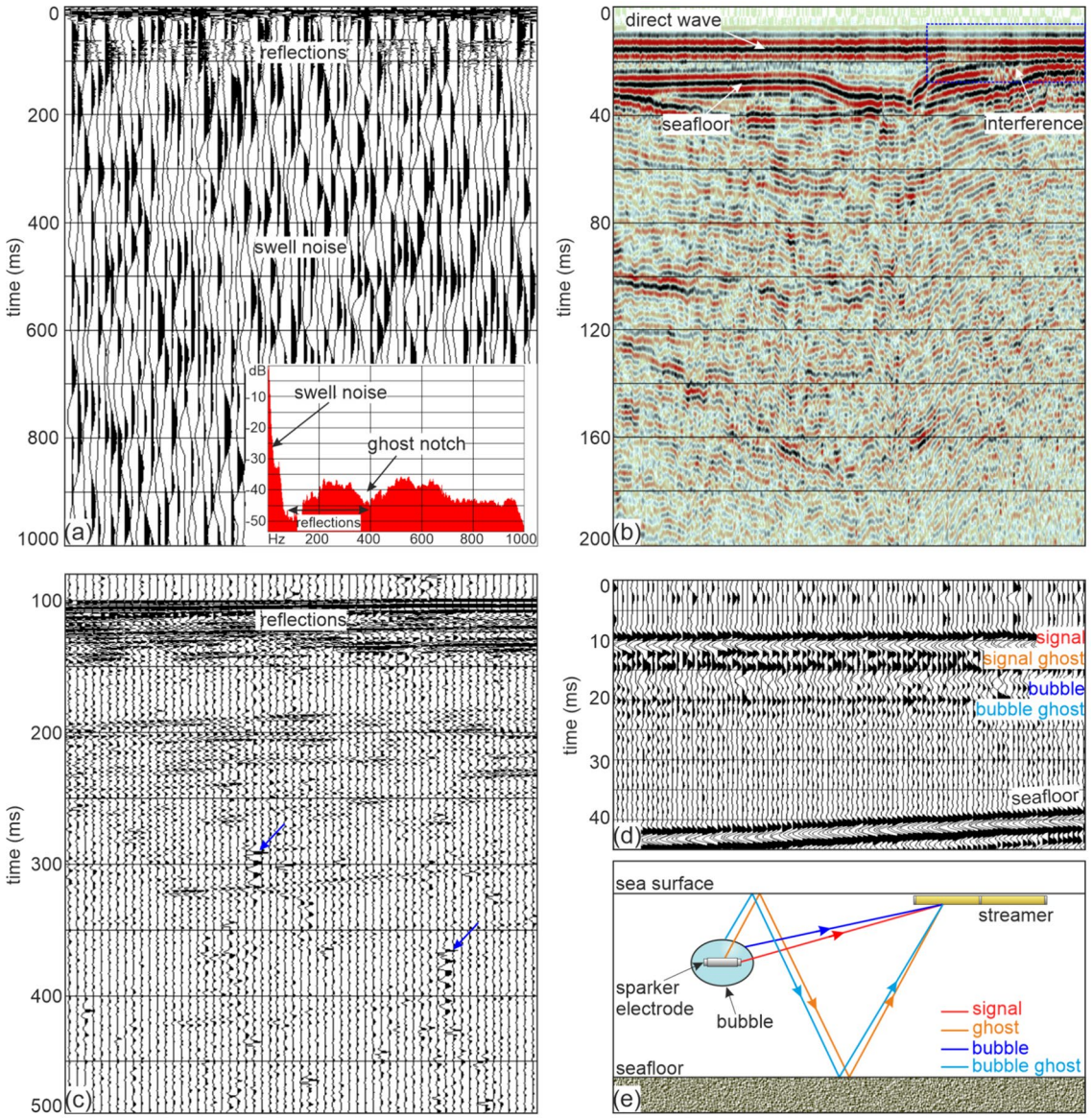

Fig. 1 Typical noise examples observed in the sparker seismic data. **a** Swell noise, **b** interference between direct wave and the seafloor reflection, **c** spike-like noise (blue arrows), **d** primary signal, ghost reflection, bubble effect, and ghost reflection of the bubble on the direct wave, and **e** schematic representation of the ray paths of the signals in (**d**). Inset in (**a**) represents the average amplitude spectrum of the data

low frequencies are also required during the inversion of seismic data for acoustic impedance. In addition, Dondurur and Karslı (2012) stated that low-frequency components are particularly important in high-resolution marine seismic surveys, because the overall signal penetration is relatively low since these surveys employ higher frequencies. Moreover, both low- and high-frequency components are required to improve the seismic resolution (Yılmaz 2001). Therefore, loss of the low frequencies may result in lower resolution in the deeper parts (Dondurur and Karslı 2012).

Multiple reflections

When the seismic signal travels the same ray path multiple times in the water column, it gives rise to multiple reflections known as reverberations. Various methods and approaches have been developed for removing multiple reflections from multi-channel seismic data. Among these, the stacking process is one of the most effective methods for suppressing multiple reflections. One of the oldest multiple suppression techniques used in conjunction with the stacking process is predictive deconvolution which suppresses multiple reflections based on the periodicity of multiples in the seismic data (Robinson and Treitel 1967).

Since the stacking process cannot be applied to single-channel sparker seismic data, multiple reflections are often retained in the final single-channel seismic sections as recorded. Therefore, the removal of multiple reflections in sparker data is still a significant challenge in engineering studies. Today, the method that can be employed for removing multiples from single-channel seismic data is predictive deconvolution, which is the only suitable method for 1D models.

Direct waves

The direct wave occurs when the seismic signal emitted from the source travels along the sea surface and reaches the streamer. These are the first signals reaching the receivers and are observed in multi-channel seismic data as events that linearly extend above the seafloor reflections in shot gathers. In sparker profiles, the distance between the sparker electrode and the streamer is quite small, generally less than 10 m. Therefore, in sparker data, direct wave appears at very early arrivals and are horizontally observed throughout the section (as long as the source–streamer spacing remains constant along the profile) (Fig. 1b). The waveform of the direct arrival in sparker data provides information about the signal quality generated by the sparker source, and a consistent direct arrival wave from trace to trace indicates that the sparker source is operating properly producing a similar seismic signal for each shot (Wang et al. 2019).

In areas where the water depth is very shallow, especially if the water depth is less than twice the source–streamer spacing, direct arrival waves will have same arrival times as the seafloor reflection, interfering and degrading the primary reflections (Fig. 1b). In such cases, it may not be possible to remove direct waves from the data through a muting process. This situation is a significant factor limiting the use of sparker systems in shallow waters, and efforts can be made to reduce this effect by decreasing the source–streamer offset.

Spike-like noise

High-amplitude, transient noise interferences are typically caused by current leaks in the seismic recorder and streamer electronic circuits in the seismic data. In liquid streamers, high-amplitude noise interferences can also be observed in seismic data in case of seawater leakage into the streamer. Spectral analyses reveal that the amplitudes of such noises spread across the entire frequency band of the seismic data, making it impossible to filter them out with simple frequency filters (Dondurur 2018).

Sparker systems use high-voltage electrical discharge in seawater to produce seismic signal, and high-amplitude spike-like noise due to the current leakage can be widely observed in the sparker data (Fig. 1c). To minimize such noise, grounding of sparker source, streamer, and recording system components is essential during data acquisition. However, despite these precautions in the acquisition, spike-like noise, especially in late arrivals where reflection amplitudes are small, can still be encountered in the sparker data. Typically, to remove this noise in the processing stage, methods such as surgical muting or alpha-trimmed trace mix can be applied. It is crucial to remove spike-like noise from sparker data before the migration process; otherwise, due to their high amplitudes compared to primary reflections, numerous semi-circular events (smiles) arise after the migration process.

Bubble effect

Discharging a high-voltage electric current into the conductive seawater generates a vapor bubble and a sound wave outward from the electrode tips (Kluesner et al. 2019; Duchesne et al. 2007). The initial vapor bubble collapses immediately after formation due to its relatively low internal pressure, creating an additional sound signal named the bubble signal. This collapse process forms sequentially diminishing bubble pulses, and each successive bubble formation and collapse creates a new pressure wave. These unwanted signals occur immediately after the primary signal, contributing to the short-path multiple reflections by adding to the primary seismic signal (Buogo and

Cannelli 2002). As a result, a mixed-phase sparker source signature is produced with a relatively long time length. Ultimately, the direct wave of this long source signal may interfere with the seafloor reflection in shallow water surveys (Fig. 1b). In sparker data, only the first bubble signal is typically distinguishable (Kluesner et al. 2019). Factors such as changes in salinity in seawater, variations in source depth due to the rough sea conditions, fluctuations in the power supply, and electrode corrosion can affect the formation, shape, and collapse time of bubble signals in sparker data, creating variability between shots. As the power of the sparker source increases, the time interval between primary and the bubble signal also increases, and the amplitude of the bubble signal approaches that of the primary signal (Mosher and Simpkin 1999; Kluesner et al. 2019).

In sparker data, the effects of the primary signal and bubble appear as sequential signals (Fig. 1d and e). Eliminating the bubble effect from sparker records is not possible during data acquisition, and wavelet data processing is required to remove this noise. For this purpose, generally, the predictive deconvolution process is applied to the seismic data.

Ghost reflection

Ghost reflections occur when the signal generated by the sparker source travels upward, reflects off the seawater/air interface, and then acts like a primary signal by reflecting from sub-bottom interfaces and reaching the receivers. Ghost reflections produced in this manner closely follow the primary signal in terms of time and are added to the end of the signal. As a result, periodic frequency gaps, known as ghost notches, appear in the frequency spectrum of the seismic record, significantly reducing the vertical resolution of the seismic data (Fig. 1a) (Dondurur 2018; Wang et al. 2019).

Generally, the usable frequency band of sparker seismic data is limited to the first ghost notch created by the ghost reflection in the spectrum (Fig. 1a). Therefore, the tow depth of the sparker source determines the bandwidth of the seismic signal recorded, where shallower tow depths produce signals with wider bandwidth and deeper tow depths yield lower-frequency signals. In sparker data, ghost reflections appear as consecutive signals along with primary signal and bubble effects, depending on the source depth and source power (Fig. 1d and e). Removing the ghost reflections from the data significantly enhances the vertical resolution. Therefore, different specific methods in addition to predictive deconvolution to eliminate the ghost reflection during the processing stage have been developed (e.g., Vakulenko et al. 2014; Provenzano et al. 2020; Egorov et al. 2017; Zhang and Masoomzadeh 2018).

Random noise

In the processing of multi-channel seismic data, stacking itself is the most effective noise suppression method for removing random noise from the data. However, single-channel seismic data do not benefit from this advantage of stacking. Therefore, suppressing both random and coherent noise in single-channel seismic data and increasing the S/N ratio are significant challenges. Especially for the suppression of random noise in sparker seismic data, specific noise suppression methods such as weighted trace mix or F-X prediction filter (F-X decon) are often applied.

Powerline harmonic noise

Harmonic noise of 50- or 60-Hz frequency from the power transmission line can be observed in marine seismic data, particularly due to interference from the seismic vessel's electrical system. This noise typically appears in the spectrum of the data as high amplitudes at 50 Hz and its multiples (Karslı and Dondurur 2018). Since sparker systems produce seismic signals through electrical discharge, noise from power transmission line can also be observed in sparker data. To mitigate the impact of this noise, all recording components should be properly grounded. However, harmonic noise occurring at 50 Hz and its multiples, can still exist in the sparker data. To remove this noise, notch filters that suppress amplitudes in a narrow frequency band (e.g., between 48 and 52 Hz) can be applied. However, such filters may incorporate gaps in the amplitude spectrum, leading to issues during deconvolution. Therefore, as a general practice, band-pass filters applied to raw sparker data with a low-frequency cut-off around 60 Hz. This ensures the removal of both low-frequency swell noise and powerline harmonic noise from the data.

Data

In this study, data processing applications were performed on single-channel sparker datasets collected from the shallow waters of Aegean Sea. The sparker data used in the applications were collected using SIG2Mille multi-tip sparker source. Data acquisition parameters are provided in Table 1. A source power of 2000 J was used, and the sparker electrode was towed from a depth of 0.5 m. In data acquisition, a single-channel surface-tow streamer with a length of 17 m was used. The vessel speed during the data acquisition was kept constant at 4 knots. The source was fired every 2 s (approximately corresponding to 4-m shot interval), and the record length was 1 s. Sampling rate of the recorded

Table 1 Data acquisition parameters for the single-channel sparker data used in the applications

Parameter	Value
Source type	SIG2Mille Multi-tip Sparker
Source power	2000 J
Sparker electrode depth	0.5 m
Streamer length	17 m
Streamer depth	Surface
Sampling rate	0.5 ms
Record length	1.0 s
Shot interval	2.0 s (~4 m)
Seismic recorder	Triton SBlogger
Lateral offset	5 m
Inline offset	0 m
Tow distance	20 m

data was 0.5 ms, which corresponds to 1000-Hz Nyquist frequency. The collected seismic data were processed using SeisSpace/ProMax software.

Processing of Sparker seismic data

Processing single-channel sparker data is not as complex and time-consuming as processing multi-channel seismic data. The data processing steps typically involve basic processes such as removing low- and high-frequency noise, muting, deconvolution, and migration. Depending on the type and amount of noise components in the data, specific methods such as trace mixing and F-X prediction filter can be included in the processing. Figure 2 illustrates the proposed data processing flow used in the processing of single-channel sparker seismic data. The important part of this flow is that it includes different processing steps for different noise types along with their specific processing parameters, for instance, f-k filter for coherent noise, F-X prediction filter for random noise, or trimmed trace mix for spike-like noise bursts, etc.

Data loading

The process of loading raw sparker seismic data into the data processing system is referred to as "data loading" and also involves a conversion of the raw data format to the internal format of the data processing software. After data loading, the header information of the loaded raw data is checked, and the accuracy of essential information for data processing, such as the shot number (Field File ID Number, FFID) and sampling rate, is confirmed. At this stage, necessary header information (e.g., CDP and channel numbers, offset value, etc.) is added to the trace header of the data if not present in the header section.

Spectral analysis and band-pass filter

Generally, seismic data consist of a linear summation of signal and noise components, including high-frequency random noise and low-frequency swell noise. Therefore, it is often necessary to filter both high- and low-frequency amplitudes from the raw seismic data using a band-pass filter. Spectral analysis is first applied to the data for this process, and the cut-off frequencies of the band-pass filter are then determined.

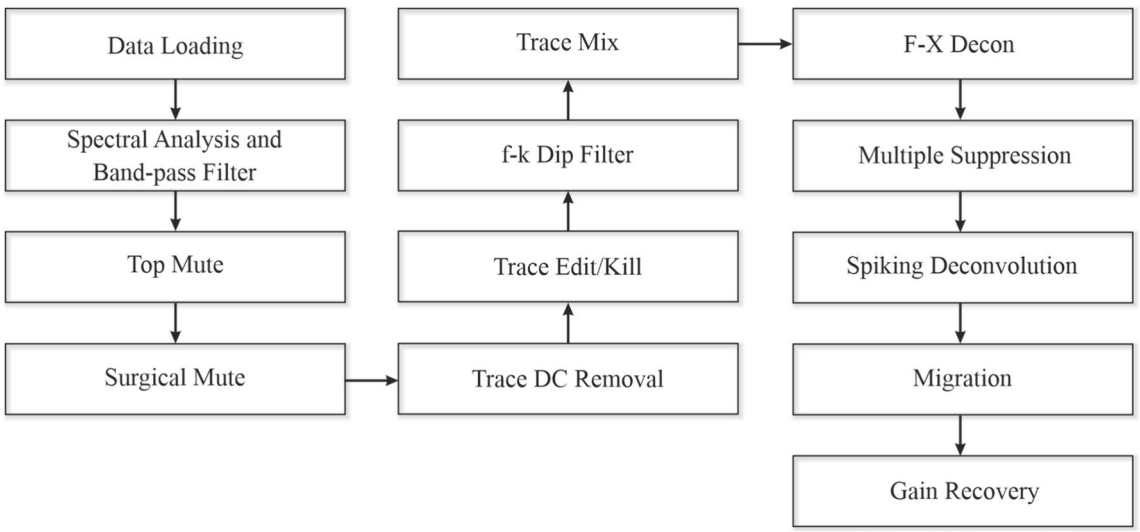

Fig. 2 Proposed data processing flow for the optimal processing of single-channel marine sparker seismic data

Sparker data typically include dominant swell noise components below 50 Hz (Fig. 3a). Although the amplitude of this noise is extremely high, the frequency band is generally lower than the sparker signal frequency band and, therefore, it can be separated from reflection signals. Raw sparker data should also be limited in the high-frequency part of the spectrum due to the ghost reflection interference. Accordingly, the usable frequency band of the seismic data is the portion between the frequency where swell noise amplitudes die and the frequency where the ghost notch is observed (Fig. 3a). Both frequency values are determined from the average amplitude spectrum of the sparker data using spectral analysis.

The filter operator length is an important parameter for the performance of the band-pass filter. Too short filter operators leave residual swell noise amplitudes in the data. On the other hand, an excessively long operator length will unnecessarily extend the processing time. Therefore, tests can be conducted on this parameter to determine the most appropriate operator length. Figure 3 shows raw single-channel sparker data before and after the band-pass filter and their corresponding amplitude spectra. Prior to the filtering, spectral analysis was used to examine the frequency content of the data, and the cut-off frequencies for the band-pass filter were determined. The high-amplitude swell noise extends up to 80 Hz in the amplitude spectrum of the raw seismic data. Additionally, the spectrum shows that the first ghost notch is around 400 Hz. Accordingly, suitable cut-off frequencies for the band-pass filter for this single-channel sparker data in Fig. 3a were determined as 80–420 Hz. The filter operator length was set at 400 ms. After filtering, the seismic data only contain the amplitudes of frequency components within the passband of the filter (Fig. 3b).

Top mute

The regions where coherent noise is observed in the data are simply multiplied by zero. The top mute process involves removing all events recorded in the water column before the seafloor reflection. With this process, direct waves in sparker data, along with subsequent ghost reflections and bubble effects in the water column, are removed. Figure 4a illustrates the top mute process applied to the sparker data given in Fig. 3b.

The only parameter to be determined for the top mute is the ramp of the mute transition zone. In the mute process,

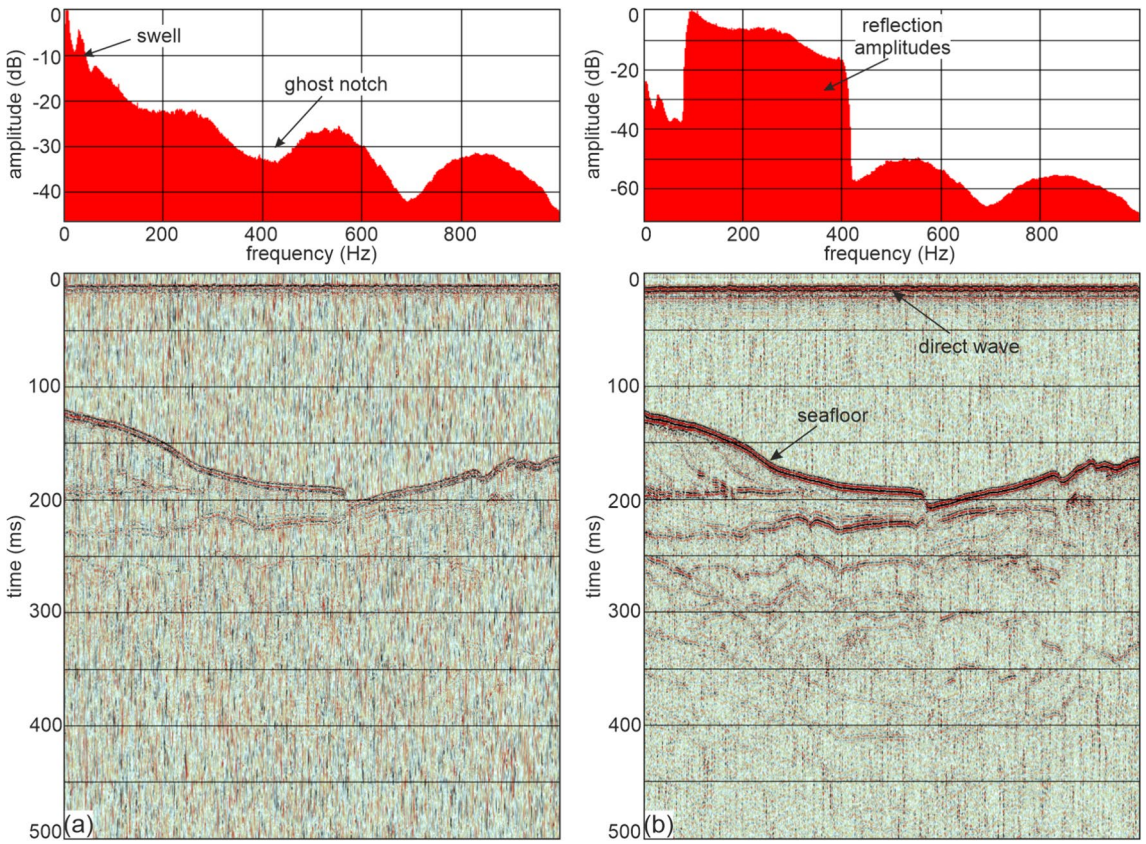

Fig. 3 **a** Raw sparker data and **b** after applying an 80–420 Hz band-pass filter. The corresponding amplitude spectra of the seismic profiles are provided at the top of the sections

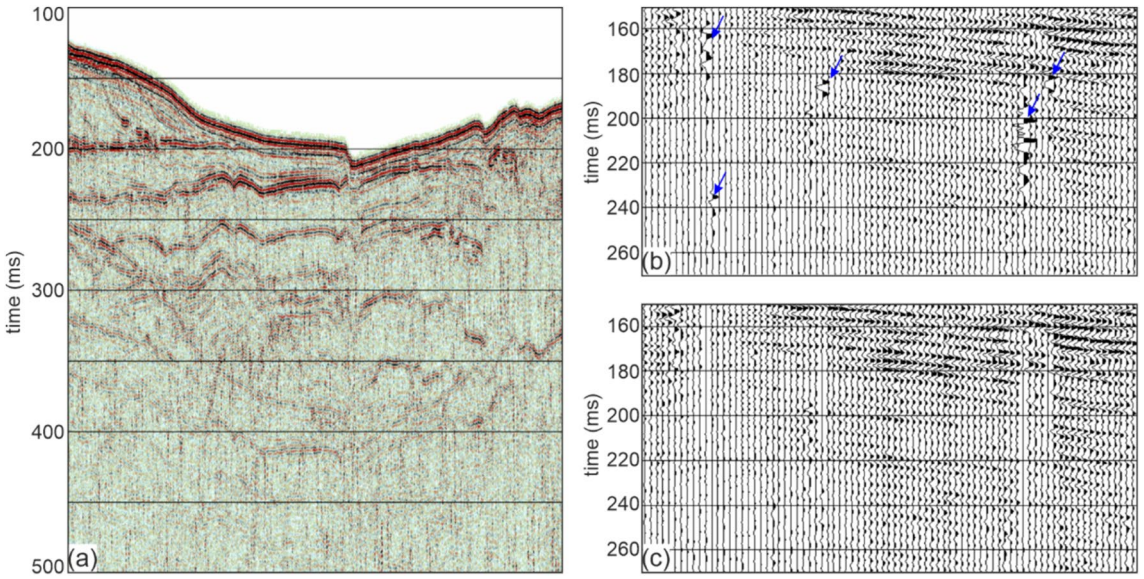

Fig. 4 **a** Sparker data shown in Fig. 3b after top mute process. **b** Close-up of spike-like noise (blue arrows) and **c** removal of this noise after applying the surgical mute

the part to be muted immediately above the seafloor is multiplied by 0, and the part to be retained in the data is multiplied by 1. For the transition zone just above the seafloor, an inclined transition zone should be defined to prevent the occurrence of Gibbs phenomenon in subsequent data processing steps. Since sparker data are high resolution, and a smaller sampling interval compared to standard multi-channel seismic data (e.g., 1 or 2 ms) is chosen for appropriate Nyquist frequency (generally 0.25 or 0.5 ms), the transition zone for the top mute process should be relatively narrow. Otherwise, amplitude of the seafloor reflection may be reduced after muting.

Surgical mute

The surgical mute involves removing the noisy portions observed in the inner part of the data (below the seafloor reflection). For sparker data, this process is typically applied to remove high-amplitude transient spike-like noise. The time window, in which the spike noise is observed, is picked, and this interval is multiplied by 0. Figure 4b illustrates sparker data containing spike-like noise (blue arrows), and Fig. 4c shows the result of applying the surgical mute process. Since the regions where the surgical mute will be applied need to be manually determined and picked for each noise region, this process can be quite time-consuming. Additionally, after the process, the amplitudes of the muted portions in the section are zeroed out. To overcome this, it is recommended to apply trace mixing to the data after the surgical mute.

Trace DC removal

The component corresponding to 0-Hz frequency in the amplitude spectrum is referred to as "DC component." This component, exhibiting no oscillation, is added to the entire seismic trace as a constant amplitude value due to constant voltage interference in the streamer electronics. In these cases, the seismic amplitudes oscillate around a constant positive or negative value away from the 0 axis. Removing the DC component from the traces is typically done by subtracting the average value of the seismic trace from each seismic sample value. Figure 5 shows an example sparker data before and after DC component removal.

Trace edit/kill

All seismic traces recorded as the seismic data may not be practically usable in some cases due to their high noise levels. In such cases, the trace in question is simply zeroed out. This process is typically applied to sparker data in the following situations:

- If the trace belongs to a missed shot
- If the trace contains excessive amount of powerline noise
- If the trace contains high amount of spike-like noise
- If there is static time shift in the trace

Trace edit is generally required in sparker data when there are traces from missed shots. The issue often arises due to triggering problems with the sparker source. Figure 6 illustrates a sparker section containing missed shots and after

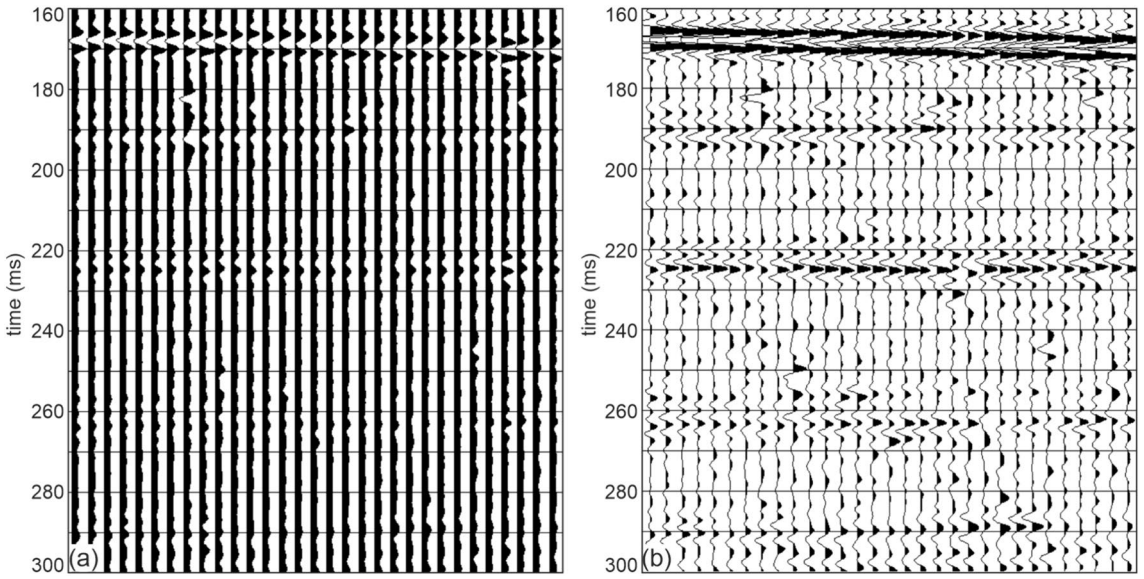

Fig. 5 Example sparker data **a** before and **b** after DC component removal. After trace DC removal, each seismic trace oscillates around the 0 axis value

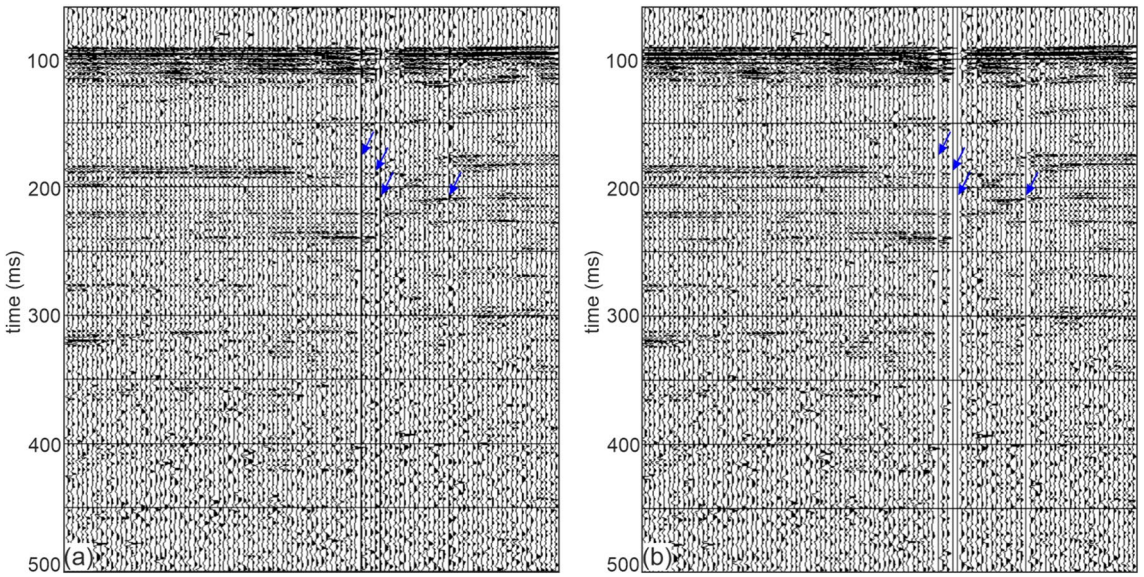

Fig. 6 **a** Example sparker data containing missed shots (blue arrows) and **b** after trace edit process

killing those traces. The amplitudes of the killed traces are zeroed out. To prevent the zero-amplitude traces in the final processed section, it is recommended to apply trace mixing to the sparker data after the editing process.

f-k dip filter

Seismic sections are comprised of different events with different slopes. Events with different slopes interfering within the seismic sections can be separated from each other through 2D Fourier transformation, and events at undesired slopes can be removed from the data using an f-k filter in the 2D Fourier domain. The general purpose of the f-k filter is typically to eliminate linear events from the data, such as tail buoy noise or operational noise. For sparker data, the f-k filter is applied when it is necessary. Figure 7 shows the single-channel sparker section shown in Fig. 4a before and after the application of the f-k filter. In the zero-offset sparker data, the amplitudes of primary reflections typically exhibit a tendency to accumulate along the 0 wavenumber

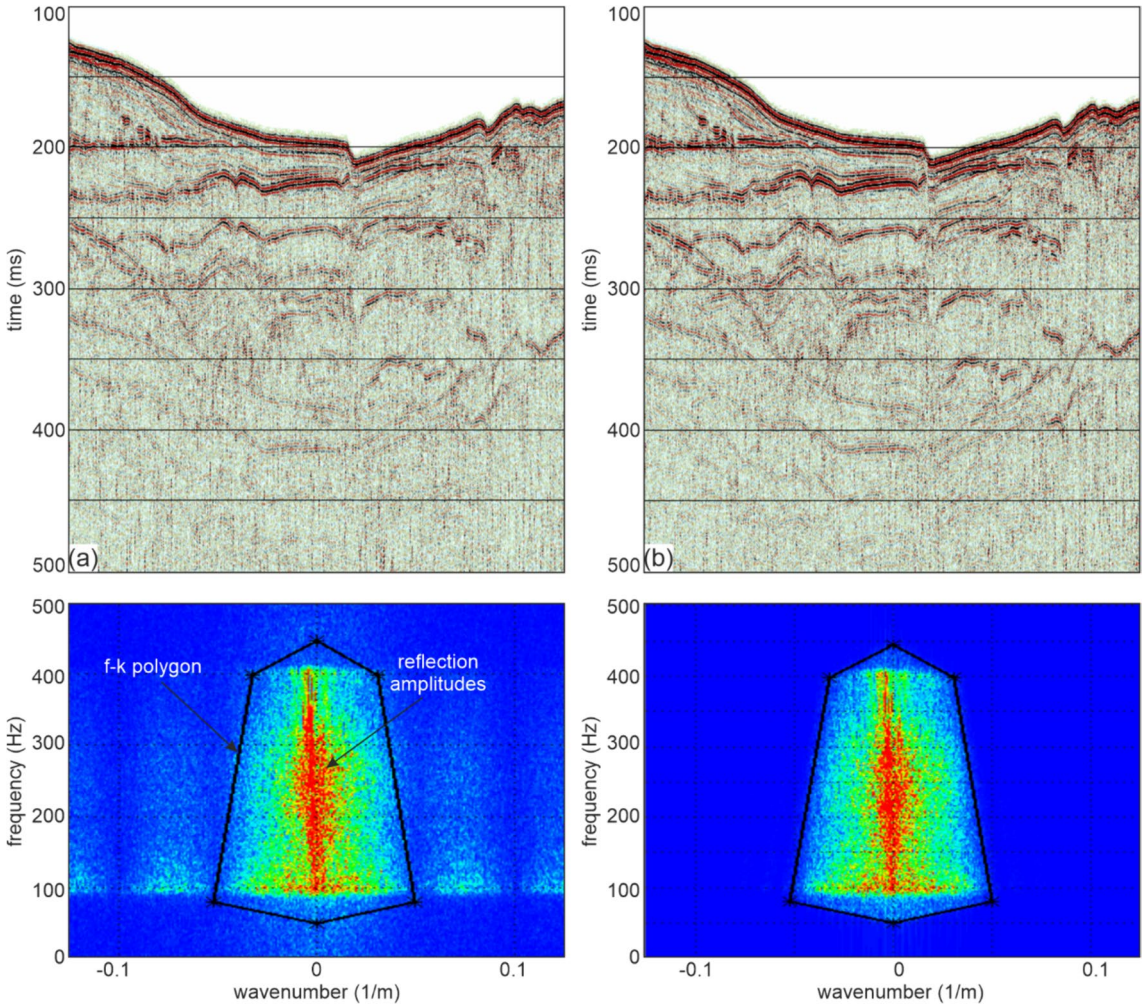

Fig. 7 **a** Sparker data shown in Fig. 4a and b after f-k filter application. Corresponding f-k panels of the profiles are provided beneath the sections

(central) axis. However, coherent linear noise amplitudes appear both at the negative and positive panels of the f-k plane. Therefore, such coherent noise can be eliminated from the data with an f-k filter that preserves amplitudes along the 0 wavenumber axis while suppressing amplitudes in other sections. In order to remove the noise amplitudes, an f-k polygon is picked, which encloses the primary reflection amplitudes (Fig. 7a). The amplitude values within the polygon are multiplied by 1.0 while the amplitudes outside of the polygon are zeroed out. After the inverse 2D Fourier transform, the seismic data contain only amplitudes in the picked polygon of the f-k plane (Fig. 7b).

Trace mix

Trace mixing, commonly applied to zero-offset sections, constitutes a noise suppression and S/N ratio enhancement method. In this method, the amplitude samples of a specific number of adjacent traces are summed, and a resultant trace is obtained by simply averaging them. The process can be implemented as weighted or trimmed trace mix. For sparker data, trimmed trace mix is often employed. In this procedure, after sorting the amplitude samples in ascending order, a certain percentage of the high and low amplitudes at both ends of this ordered series is excluded from the average.

Trace mixing can be conceptualized as a horizontal stacking method and can be effectively employed as a noise suppression and S/N ratio enhancement tool for single-channel sparker sections where random noise cannot be suppressed through stacking. Additionally, it can be utilized in interpolating missing traces as well as samples resulting from the trace editing and surgical mute process of single-channel seismic data. Trimmed trace mix is highly effective and practical method for automatically removing spike-like noise observed in the sparker data. Figure 8a shows a part of an example single-channel sparker section containing several

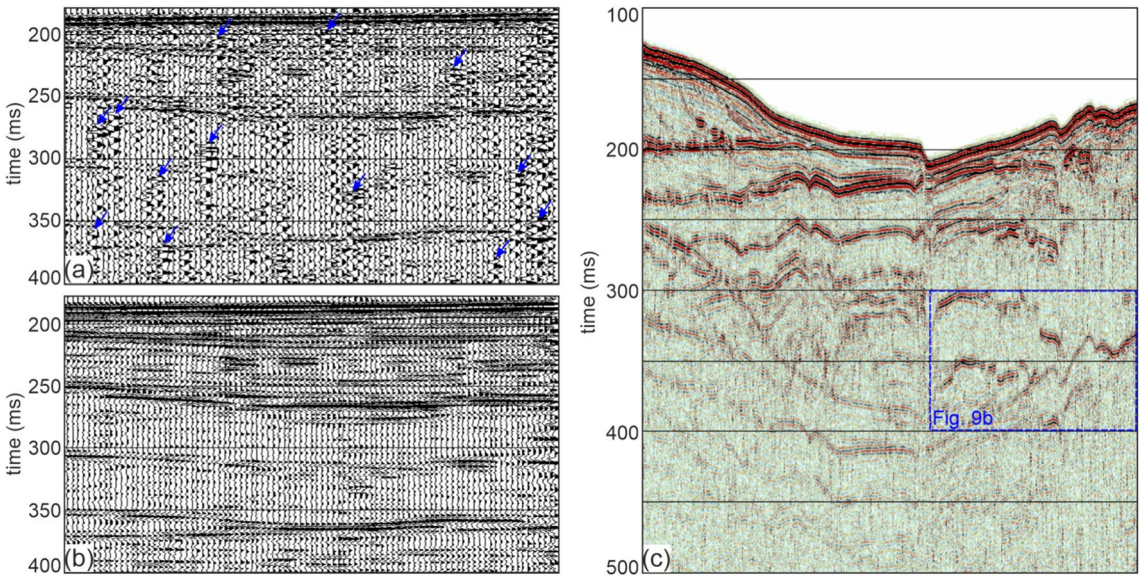

Fig. 8 **a** A part of an example sparker section with spike-like noise bursts (blue arrows) and **b** after the 20% trimmed trace mix. **c** Result of 20% trimmed trace mix applied to the sparker data shown in Fig. 7b

high-amplitude spike-like noise bursts. After 20% trimmed trace mix, all high-amplitude spike-like noises, indicated by blue arrows, have been removed from the data, and trace-by-trace consistency is significantly improved (Fig. 8b). Figure 8c shows the result of 20% trimmed trace mix applied to the sparker data shown in Fig. 7b.

F-X prediction filter (F-X decon)

F-X prediction filter is an effective technique for random noise suppression, relying on time–distance prediction over small windows in seismic data. The difference between the predicted and actual waveforms is considered as noise and subtracted from the data. The F-X prediction filter is typically applied to post-stack or single-channel seismic data because the stacking process inherently suppresses a significant portion of the random noise amplitudes. However, in the case of single-channel sparker data where stacking cannot be applied, random noise amplitudes can be relatively high especially in late arrivals where the reflection amplitudes are relatively small. In such cases, the F-X prediction filter can be employed to increase the S/N ratio of sparker seismic data. If we define a window which is small enough both in spatial and temporal directions, the nonlinear events can be considered as linear, and hence, they can be predicted in f-x domain. Figure 9a shows the F-X prediction filter application to the sparker data shown in Fig. 8c. For this data, the time length of the filter is 1000 ms, and the horizontal window width is 200 traces. The effectiveness of the F-X prediction filter in suppressing random noise is significant particularly in the late arrivals of the sparker data (Fig. 9b and c). The amplitude spectra of the close-ups clearly illustrate the amplitudes of random noise removed by the F-X prediction filter (Fig. 9d and e).

Gain recovery

The amplitude of the seismic signals traveling away from the source diminishes with distance due to the specific effects such as spherical divergence and absorption, which require amplitude enhancement using appropriate gain functions. One of the most commonly employed gain control methods in the seismic data processing industry is known as automatic gain control (AGC). As AGC eliminates the relative amplitude changes from trace to trace in seismic data, it is not utilized in hydrocarbon analyses of the seismic profiles. If seismic data are analyzed for subsurface structural information, such as fault mapping, AGC facilitates interpretation by equalizing shallow and deeper amplitude levels.

In this study, AGC is applied to sparker data only for display purposes. The most critical parameter that needs to be appropriately chosen in AGC is the window length. As the window length decreases, AGC becomes more effective, and amplitudes in both shallow and deep regions of the data become more balanced. In practice, the suitable window length is selected based on the record length of the input data. Since the record length of sparker data is generally much shorter than that of multi-channel seismic data, relatively shorter AGC window lengths should be preferred for sparker profiles. Figure 10a shows the result of applying AGC to the sparker data given in Fig. 9a using a

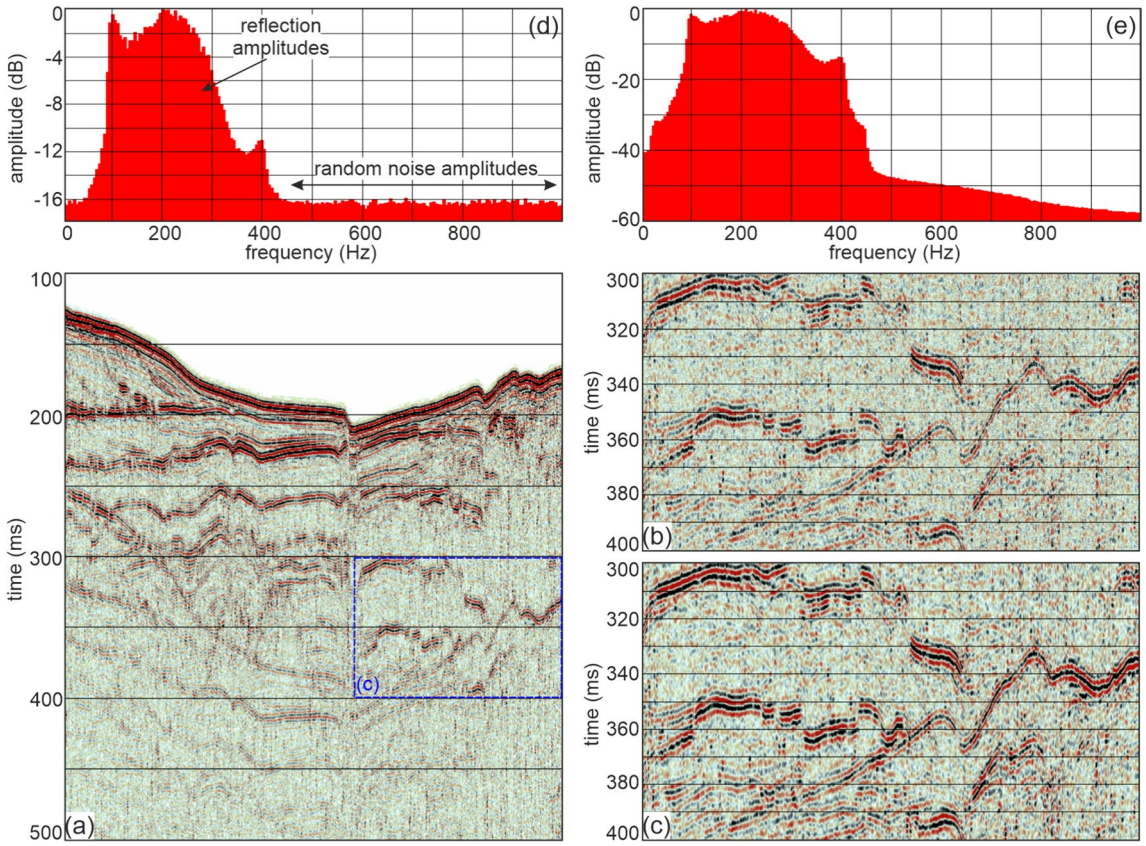

Fig. 9 **a** F-X prediction filter result of the sparker data shown in Fig. 8c. **b** and **c** show the close-ups of the deeper parts of the data before and after applying the F-X prediction filter, respectively. Corresponding average amplitude spectra of the close-ups before and after the filter are given in (**d**) and (**e**), respectively

75-ms window length. In the AGC output, the amplitudes at shallow and deep parts of the seismic section seem to be balanced.

Multiple suppression

Multiple reflections in marine seismic data can pose significant challenges during the interpretation of the data collected with short streamers in relatively shallow waters. While various methods have been proposed to predict and suppress multiple reflections, these techniques (except predictive deconvolution) are effective on multi-channel seismic data only. Therefore, predictive deconvolution was employed to eliminate multiple reflections from single-channel sparker data in this study.

Predictive deconvolution allows obtaining the time-advanced version of the input trace. If the input trace is s(t), its time-advanced version is s(t + α), where α is referred to as the "prediction lag." In deconvolution, the determination of prediction lag (α) and operator length (n) parameters is crucial. The maximum attenuation in the amplitudes of multiple reflections is achieved when the prediction lag is equal to the period of the multiple reflections, regardless of the operator length. The period of multiple reflections as well as the appropriate prediction lag value to suppress the multiples can be found by analyzing the autocorrelation of the input seismic data. To eliminate the multiple reflections from the data, the operator length should be chosen long enough to encompass the first isolated energy packet in the autocorrelation. Figure 10b shows the result of applying predictive deconvolution to the sparker data given in Fig. 10a. The autocorrelations of the sections are also presented beneath the sections. In the deconvolution process, the prediction lag ($\alpha = 120$ ms, water depth dependent) and operator length ($n = 30$ ms) were selected. It is observed that predictive deconvolution successfully suppresses multiple reflections in the sparker data particularly originated from the seafloor.

Spiking deconvolution

Spiking deconvolution is applied to enhance temporal resolution and eliminate the bubble effect as well as ghost reflections. Because sparker data are inherently mixed-phase, and spiking deconvolution is typically applicable

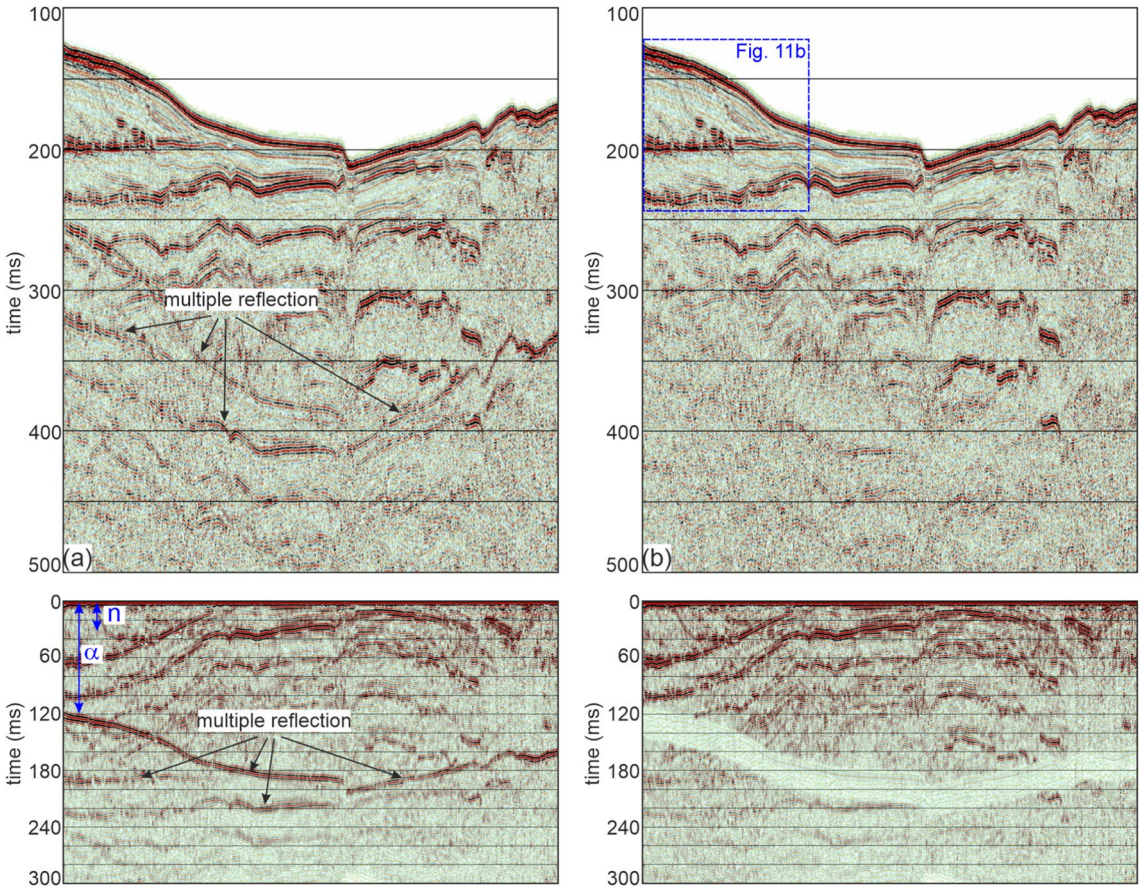

Fig. 10 **a** Sparker data shown in Fig. 9a after applying AGC using a 75-ms window length and **b** after predictive deconvolution application ($\alpha = 120$ ms and $n = 30$ ms) to the section in (**a**). Corresponding autocorrelations of the profiles are presented beneath the sections. AGC is applied to sparker data in (**a**) only for display purposes, and the predictive deconvolution is applied to sparker data with no gain

only for minimum-phase data, it is necessary to first convert the data to its minimum-phase equivalent before applying spiking deconvolution. Figure 11 illustrates the application of spiking deconvolution to the single-channel sparker data given in Fig. 10b. In this study, the sparker data were transformed to its zero-phase equivalent, instead of minimum-phase, before applying zero-phase spiking deconvolution to the entire section. The operator length for the deconvolution process is chosen as $n = 30$ ms. The effectiveness of the process in eliminating ghost reflections and bubble effects in the data is particularly evident in the close-ups presented in Fig. 11b and c. The clinoforms of the delta structure, concealed by ghost reflections and bubble effect that extends parallel to the seafloor reflection (indicated by blue arrows in Fig. 11b), are now much clearer after deconvolution. The average amplitude spectra of the seismic sections before and after deconvolution are shown in Fig. 11d and e, respectively. From the spectra, it can be observed that spiking deconvolution enhances the amplitudes of high-frequency components, particularly between 300 and 400 Hz.

Migration

As they are zero offset, post-stack time migration algorithms can be applied to single-channel sparker seismic data. Although there are several migration algorithms used in the seismic data processing industry, the most commonly used for sparker data are Stolt and Kirchhoff time migrations. All migration algorithms require knowledge of the seismic velocity of the subsurface. However, obtaining the velocity distribution of the subsurface from single-channel sparker data is not possible. Therefore, constant velocity migration is typically applied to sparker data, assuming a seismic wave velocity of 1500 m/s for whole seismic section. Figure 12 illustrates the sparker data shown in Fig. 11a after Stolt and Kirchhoff migrations. Applications demonstrate that, in structurally complex environments, Kirchhoff migration algorithm makes the fault planes more distinct. However, for the shallow subsurface which is not structurally complex, both Stolt and Kirchhoff migrations produce approximately equivalent results for single-channel sparker data (Fig. 12). On the other hand, since it is the fastest and hence the most

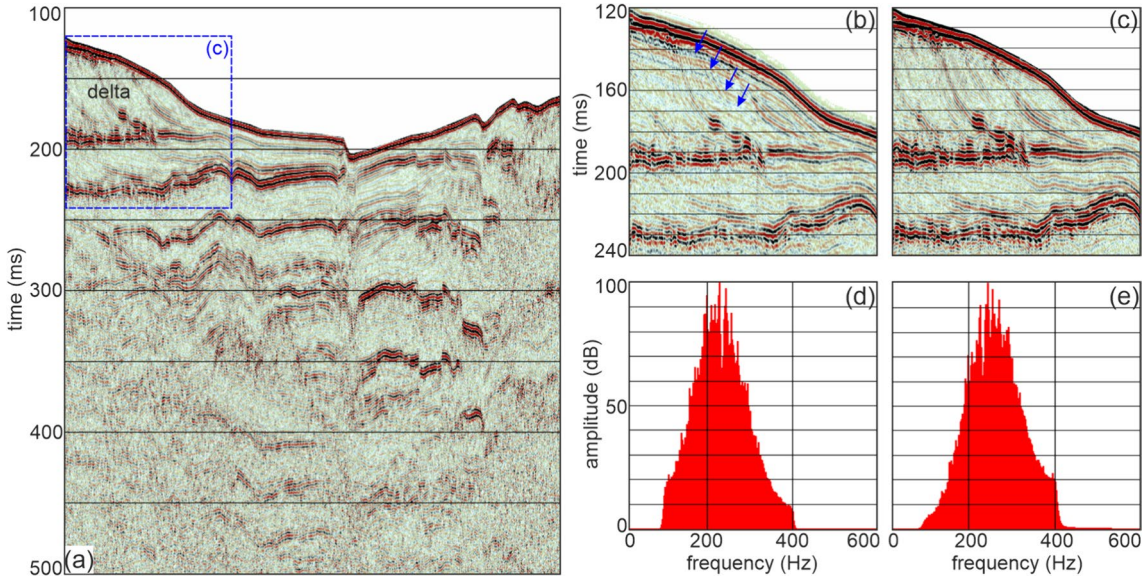

Fig. 11 **a** Sparker data in Fig. 10b after spiking deconvolution ($n = 30$ ms). **b** and **c** show close-ups of the delta structure before and after deconvolution, respectively. **d** and **e** are average amplitude spectra of the seismic data before and after deconvolution, respectively. Blue arrows in (**b**) indicate ghost reflections and bubble effect

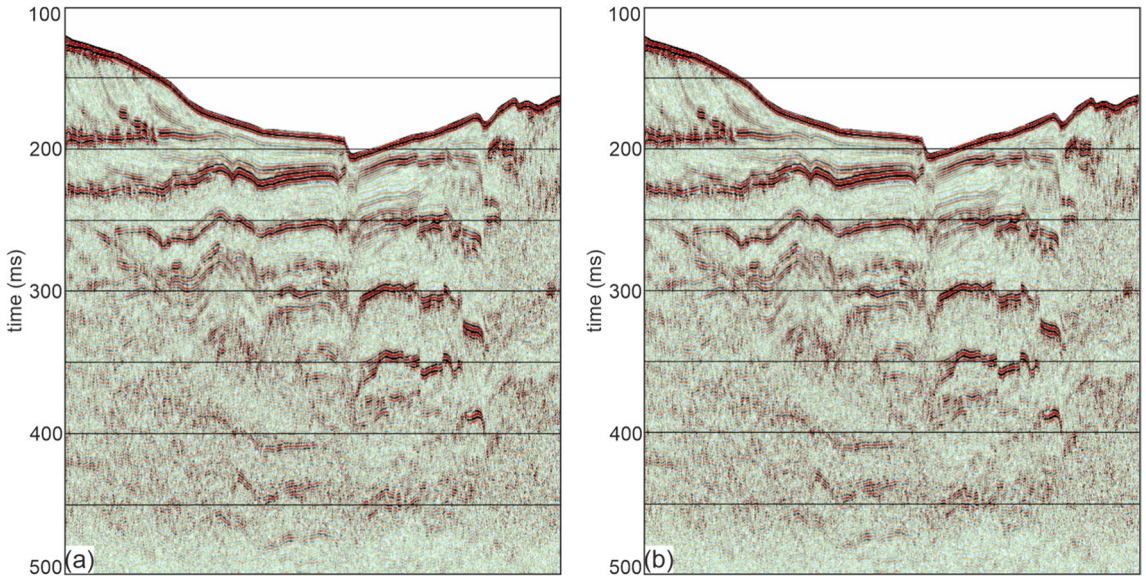

Fig. 12 The sparker data shown in Fig. 11a after **a** Stolt and **b** Kirchhoff migrations

computationally efficient algorithm, the Stolt algorithm is often preferred for processing sparker data.

Discussion and conclusions

The single-channel sparker seismic reflection systems are widely employed in marine geo-engineering studies for several reasons. These include their relatively low data acquisition costs enabling cost-effective data collection, their capacity to operate in shallow water and narrow bays, providing of high-resolution data for approximately 200 m from the seabed, and the relatively easy data processing stages. Despite similarities with the processing of multi-channel data in various aspects, such as band-pass filtering, gain application, S/N ratio enhancement, and post-stack migration procedures, the processing of sparker data represents unique challenges due to specific characteristics inherent to

the data, such as the source waveform being mixed-phase (Kluesner et al. 2019; Duchesne et al. 2007; Santos et al. 2021; Kong et al. 2012; Yang et al. 2022).

Single-channel seismic data also possess distinctive limitations. Among these are the unavailability of the most effective noise suppression method, stacking, which is routinely applied to suppress both random and coherent noise components in multi-channel seismic data such as multiple reflections (Santos et al. 2021; Dondurur 2018). However, suppressing the random and coherent noise components, as well as in enhancing the S/N ratio, may become a significant challenge in the single-channel sparker data processing with the inability to apply stacking.Multi-channel data acquisition provides the determination of the 2D velocity distribution of subsurface layers through velocity analyses applied to common depth point (CDP) gathers, which consist of traces reflecting from the same point at the subsurface but recorded at different offsets at the surface. However, due to the absence of different source–receiver offsets in single-channel seismic data, it is not possible to obtain the subsurface velocity distribution from the sparker data. This limitation becomes particularly problematic in environments with complex geology, where processes requiring the knowledge of subsurface velocity distribution, such as migration procedures, encounter difficulties when applied to single-channel seismic data.

Another limitation associated with the processing of single-channel seismic data is related to suppressing the noise content and enhancing the S/N ratio. Single-channel seismic data may contain random noise and short-period multiples (such as ghost reflections and bubble effects) that significantly constrain the resolution (Kluesner et al. 2019; Duchesne et al. 2007; Santos et al. 2021). Specifically, for effective suppression of random noise and spike-like noise, specific methods such as trimmed trace mix or F-X prediction filter are often required. Santos et al. (2021) emphasized the significant issue of random noise in their processing of sparker data, and they proposed that the predictive deconvolution process reduced the amplitudes of random noise and enhanced lateral continuity. However, the applications in this study suggest the opposite, as the deconvolution process is known to excessively boost the amplitudes of both low- and high-frequency noise in the data (e.g., Yılmaz 2001; Dondurur 2018). Therefore, in this study, band-pass filtering was applied to the data following the deconvolution, and F-X prediction filter was used to remove random noise (Fig. 9). Another significant challenge in the processing of single-channel seismic data is the presence of multiples. Several multiple reflections suppression algorithms used in the seismic data processing industry, such as surface-related multiple elimination (SRME), radon velocity filters, f-k filters, or wave equation multiple elimination (WEMR), have been developed specifically for multi-channel seismic data and require offset data acquisition. Consequently, their application to single-channel seismic is not feasible. However, the application of predictive deconvolution, which is theoretically suitable for a 1D earth model, allows for the suppression of multiples in the single-channel sparker data (Robinson and Treitel 1967; Peacock and Treitel 1969). The effectiveness of multiple suppression through predictive deconvolution relies on the periodicity of multiple reflections in the seismic data, and the multiples are periodic in zero-offset sections. However, the efficacy of the predictive deconvolution relies on the fulfillment of six assumptions made for deconvolution (Yılmaz 2001; Dondurur 2018). Since satisfying all these assumptions simultaneously is nearly impossible, predictive deconvolution may not produce perfect results in removing multiples from the data. This is evident from the residual multiple reflection amplitudes observed in the output of predictive deconvolution for the sparker data shown in Fig. 10b.

The deconvolution process itself is one of the most crucial and challenging steps in the processing of single-channel sparker data. One of the reasons for this is the proper determination of the operator length (n) and prediction lag (α) parameters in deconvolution. Both parameters are typically determined through several tests based on the autocorrelation of seismic data (Fig. 10a). If these parameters are not appropriately chosen, multiples may not be sufficiently suppressed, and the amplitudes of primary reflections may be reduced (Güney et al. 2019; Üge and Kanlı 2022). Applications demonstrate that the suppression of multiple amplitudes is maximized when the prediction lag is equal to the period of multiples (Yılmaz 2001; Dondurur 2018). In any case, the accurate determination of the deconvolution parameters can be a time-consuming process, often requiring numerous tests and trials.

The second issue related to deconvolution is the signal waveform generated by the sparker source. The Wiener–Levinson deconvolution theory is valid for minimum-phase wavelets (Robinson and Treitel 1967; Yılmaz 2001). However, the signal produced by the sparker source is mixed-phase (Kluesner et al. 2019; Duchesne et al. 2007; Santos et al. 2021; Yang et al. 2022). Therefore, the signal needs to be transformed to its minimum-phase equivalent before deconvolution. Tests conducted in this study reveal that when zero-phase deconvolution is applied to sparker data, ghost reflections and bubble effects are effectively suppressed. Hence, the waveform of the sparker data was first transformed to a zero-phase wavelet, and then, a zero-phase deconvolution was performed (Figs. 10b and 11a).

The resolution of sparker data is significantly enhanced by the removal of ghost reflections from. In this regard, it is observed that, in addition to the numerous specific algorithms developed for this purpose, spiking deconvolution substantially eliminates short-period multiples in the sparker

data, particularly ghost reflections and bubble effects, effectively removes the ringy appearance of the reflections, and increases the temporal resolution as well as S/N ratio (Fig. 11). However, the application of specific deghosting algorithms can further enhance the resolution of sparker data (e.g., Provenzano et al. 2020).

Trace mixing has been identified as a crucial data processing step that enhances the resolution and trace-by-trace consistency of the single-channel sparker data. This method can be applied as weighted trace mix to remove random noise from sparker data where stacking cannot be applied. Additionally, if there are high-amplitude spike-like noise in the data, trimmed mix can be used to mitigate spike noises effectively (Fig. 8). For trimmed mix, the ratio of traces to be excluded in the averaging process can be determined appropriately through testing.

Acknowledgements I would like to thank Dr. Derman Dondurur for his valuable contributions on the earlier version of this manuscript.

Author contributions Aslıhan Nasıf performed conceptualization, seismic data analysis, modeling, methodology, visualization, writing, review, and editing of the manuscript.

Funding Open access funding provided by the Scientific and Technological Research Council of Türkiye (TÜBİTAK). No funds, grants, or other support were received during the preparation of this manuscript.

Declarations

Conflict of interest The author has no competing interests to declare that are relevant to the content of this article.

Open Access This article is licensed under a Creative Commons Attribution 4.0 International License, which permits use, sharing, adaptation, distribution and reproduction in any medium or format, as long as you give appropriate credit to the original author(s) and the source, provide a link to the Creative Commons licence, and indicate if changes were made. The images or other third party material in this article are included in the article's Creative Commons licence, unless indicated otherwise in a credit line to the material. If material is not included in the article's Creative Commons licence and your intended use is not permitted by statutory regulation or exceeds the permitted use, you will need to obtain permission directly from the copyright holder. To view a copy of this licence, visit http://creativecommons.org/licenses/by/4.0/.

References

Alessandrini B, Gasperini M (1989) The deconvolution of marine seismic source: an iterative approach. Geophys 54:780–784. https://doi.org/10.1190/1.1442706

Bekara M, van der Baan M (2010) High–amplitude noise detection by the expectation–maximization algorithm with application to swell–noise attenuation. Geophys 75:V39–V49. https://doi.org/10.1190/1.3428749

Birinci H, Ergün K, Yavuzoğlu AZ, Köse K, Yalçın GB, Doğan MB, Karci FB, Evren M, Güngör A, Aydemir BS (2023) Noise attenuation of a 3D marine seismic reflection dataset-A case study in the southwest Black Sea region. Bull Miner Res Exp 172:31–39. https://doi.org/10.19111/bulletinofmre.1180869

Buogo S, Cannelli GB (2002) Implosion of an underwater spark-generated bubble and acoustic energy evaluation using the Rayleigh model. J Acoust Soc Am 111:2594–2600. https://doi.org/10.1121/1.1476919

Dondurur D (2018) Acquisition and processing of marine seismic data. Elsevier, Netherlands

Dondurur D, Karslı H (2012) Swell Noise suppression by Wiener prediction filter. J Appl Geophy 80:91–100. https://doi.org/10.1016/j.jappgeo.2012.02.001

Dragoset B (2000) Introduction to air guns and air-gun arrays. Lead Edge 19:892–897. https://doi.org/10.1190/1.1438741

Duchesne MJ, Bellefleur G, Galbraith M, Kolesar R, Kuzmiski R (2007) Strategies for waveform processing in sparker data. Mar Geophys Res 28:153–164. https://doi.org/10.1007/s11001-007-9023-8

Egorov A, Glubokovskikh S, Bóna A, Pevzner R, Gurevich B, Tokarev M (2017) How rough sea affects marine seismic data and deghosting procedures. Geophys Prospect 66:1–10. https://doi.org/10.1111/1365-2478.12535

Elboth T, Reif BAP, Andreassen O (2009) Flow and swell noise in marine seismic data. Geophys 74:Q17–Q25. https://doi.org/10.1190/1.3078403

Güney R, Karslı H, Dondurur D (2019) Optimum parameter selection in offset-dependent predictive deconvolution: testing on multichannel marine seismic data. Mar Geophys Res 40:601–617. https://doi.org/10.1007/s11001-019-09390-w

Herman M, Hashim HS, Latif AH, Ghosh DP (2017) Application of FK filtering for coherent noise removal in high-frequency shallow marine data. IOP Conf Ser Earth Environ Sci 88:012010. https://doi.org/10.1088/1755-1315/88/1/012010

Huang Y, Zhang L, Zhang X, Li S, Liu Z, Yan K (2015) Electroacoustic process study of plasma sparker under different water depth. IEEE J Ocean Eng 40:1029–1040. https://doi.org/10.1109/joe.2014.2382451

Jones LE (2013). High frequency enhancement of sparker sub-bottom profiles with multichannel reflection processing. In: International Geophysical Conference and Exhibition (ASEG-PESA), 1:1–4. https://doi.org/10.1071/aseg2013ab240

Karslı H, Dondurur D (2018) A Mean-based filter to remove power line harmonic noise from seismic reflection data. J Appl Geophys 153:90–99. https://doi.org/10.1016/j.jappgeo.2018.04.014

Kluesner J, Brothers D, Hart P, Miller N, Hatcher G (2019) Practical approaches to maximizing the resolution of sparker seismic reflection data. Mar Geophys Res 40:279–301. https://doi.org/10.1007/s11001-018-9367-2

Kong F, He T, Spence GD (2012) Application of deep-towed multichannel seismic system for gas hydrate on mid-slope of northern Cascadia margin. Sci China Earth Sci 55:758–769. https://doi.org/10.1007/s11430-012-4377-4

Mosher DC, Simpkin PG (1999) Status and trends of marine high resolution seismic reflection profiling: data acquisition. Geosci Can 26:174–188

Peacock KL, Treitel S (1969) Predictive deconvolution: theory and practice. Geophysics 34:155–169. https://doi.org/10.1190/1.1440003

Pei Y, Kan G, Zhang L, Huang Y, Liu Z, Liu B, Yan K (2019) Characteristics of source wavelets generated by two sparkers. J Appl Geophy 170:103819. https://doi.org/10.1016/j.jappgeo.2019.103819

Provenzano G, Henstock TJ, Bull JM, Bayrakcı G (2020) Attenuation of receiver ghosts in variable depth streamer high resolution seismic reflection data. Mar Geophys Res 41:2. https://doi.org/10.1007/s11001-020-09407-9

Robinson EA, Treitel S (1967) Principles of digital Wiener filtering. Geophys Prospect 15:311–333. https://doi.org/10.1111/j.1365-2478.1967.tb01793.x

Santos I, Gomes M, Garabito G, Vital H, Lopes V (2021) High-resolution marine seismic data processing using a single-channel sparker system: Bahia shelf, Brazil. Braz J Geophys 39:209–226. https://doi.org/10.22564/rbgf.v39i3.2095

Trabant PK (1984) Applied high-resolution geophysical methods: offshore geoengineering hazards. Int Hum Resour Dev Corp Boston 86:214–215. https://doi.org/10.1111/j.1365-246x.1986.tb01082.x

Üge MA, Kanlı Aİ (2022) Comparison of the results of the suppression of surface-related multiple reflections by predictive deconvolution in pre- and post-stack in 2D marine seismic reflection data: a case study from the Sea of Marmara. Bull Miner Res 167:51–64

Vakulenko SA, Buryak SV, Gofman PA and Finikov DB (2014). Deghosting of high resolution marine seismic data by adaptive filtering algorithm. In: Near Surface Geoscience–1st Applied Shallow Marine Geophysics Conference.

Verbeek NH, McGee TM (1995) Characteristics of high-resolution marine reflection profiling sources. J Appl Geophy 33:251–269. https://doi.org/10.1016/0926-9851(95)90045-4

Wang X, Qi B, Zhao Q, Wang W, Yu K (2019) Feasibility of sparker source in marine seismic exploration: data analysis and processing. Acta Geophys 67:1413–1418. https://doi.org/10.1007/s11600-019-00346-7

Wu Z, Yang F, Tang Y (2020) High-resolution Seafloor Survey and Applications. Springer, Singapore. https://doi.org/10.1007/978-981-15-9750-3

Yang Z, Wang X, Hao X, Qian H, Chen X (2022) Research on combined processing techniques of air gun and sparker source towed streamer seismic data. Mar Geophys Res 43:18. https://doi.org/10.1007/s11001-022-09484-y

Yılmaz Ö (2001) Seismic data analysis processing, inversion, and interpretation of seismic data. Society of Exploration Geophysicists, Houstan. https://doi.org/10.1190/1.9781560801580

Zhang Z, Masoomzadeh H (2018) Evolution of deghosting process for single-sensor streamer data from 2D to 3D. Geophys Prospect 66:975–986. https://doi.org/10.1111/1365-2478.12614

Zheng J, Xu J, Tong S, Huang Y, Zhou H (2021) Estimation of seafloor reflectivity in shallow water based on seismic data of sparker sources. Mar Geophys Res 42:33. https://doi.org/10.1007/s11001-021-09456-8